



Original Research Article

Investigating the properties of cobalt phosphate nanoparticles synthesized by co-precipitation method

Jude N. Udeh^a, Agnes C. Nkele^{a,*}, Raphael M. Obodo^{a,b,c}, Innocent C. Nwodo^a, Chinedu P. Chime^d, Assumpta C. Nwanya^{a,e,f}, Malik Maaza^{e,f}, Fabian I. Ezema^{a,e,f,g}

^a Department of Physics and Astronomy, University of Nigeria, Nsukka, 410001, Enugu State, Nigeria

^b National Center for Physics, Quaid-i-Azam University, Islamabad, 44000, Pakistan

^c NPU-NCP Joint International Research Center on Advanced Nanomaterials and Defects Engineering, Northwestern Polytechnical University, Xi'an, 710072, China

^d Department of Agricultural and Bioresources Engineering, University of Nigeria, Nsukka, Enugu State, Nigeria

^e Nanosciences African Network (NANOAFNET) iThemba LABS-National Research Foundation, 1 Old Faure Road, Somerset West 7129, P.O. Box 722, Somerset West, Western Cape Province, South Africa

^f UNESCO-UNISA Africa Chair in Nanosciences/Nanotechnology, College of Graduate Studies, University of South Africa (UNISA), Muckleneuk Ridge, P.O. Box 392, Pretoria, South Africa

^g Africa Centre of Excellence for Sustainable Power and Energy Development (ACE-SPED), University of Nigeria, Nsukka, Enugu State, Nigeria

ARTICLE INFORMATION

Received: 29 September 2021

Received in revised: 11 November 2021

Accepted: 12 November 2021

Available online: 18 January 2022

DOI: [10.48309/JMNC.2022.1.3](https://doi.org/10.48309/JMNC.2022.1.3)

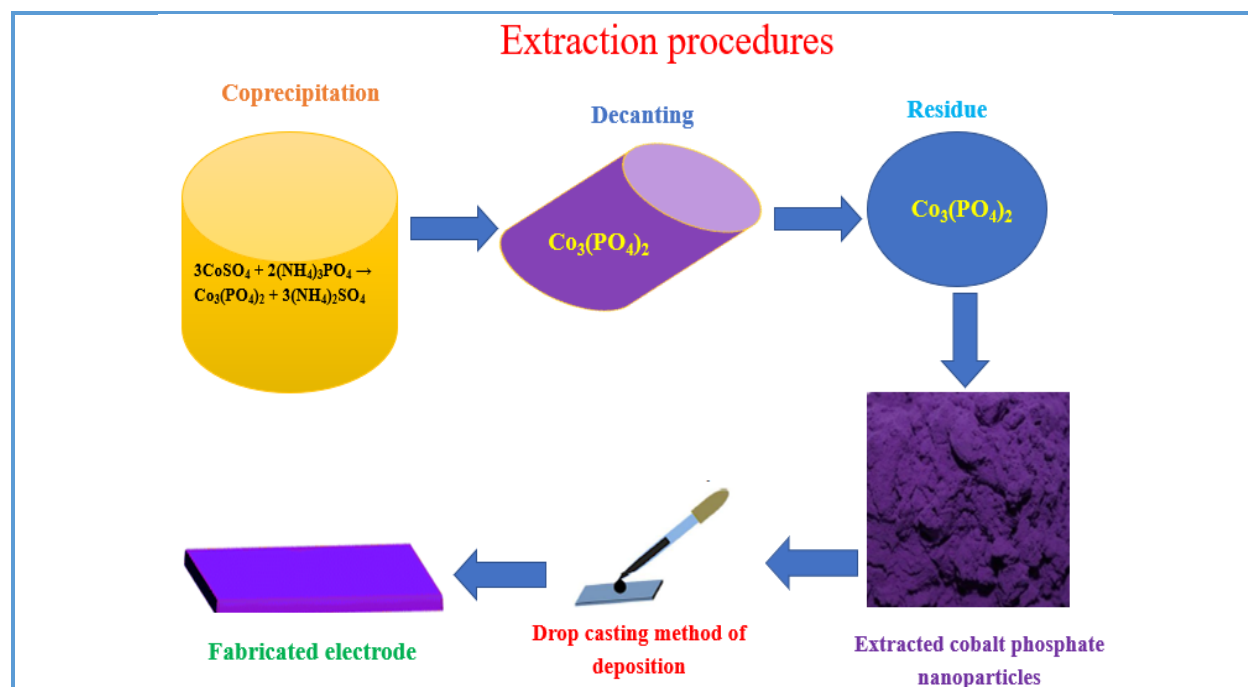
KEYWORDS

Cobalt phosphate
Coprecipitation
Drop casting
Band gap energy
Specific capacitance

ABSTRACT

Cobalt phosphate ($\text{Co}_3(\text{PO}_4)_2$) nanoparticles of varying precursor concentrations were extracted successfully by co-precipitation method and fabricated on the stainless and glass substrates using drop-casting method. The structural and morphological properties of cobalt phosphate ($\text{Co}_3(\text{PO}_4)_2$) nanoparticles were investigated by X-ray diffraction (XRD) and scanning electron microscope (SEM) techniques. Elemental composition of cobalt phosphate nanoparticles was evaluated using energy dispersive X-ray spectroscopy (EDS). The optical properties of cobalt phosphate ($\text{Co}_3(\text{PO}_4)_2$) nanoparticles were characterized using UV visible spectrophotometer. The electrochemical analyses were assessed using three-reference electrode potentiostat. XRD characterization of the cobalt phosphate nanoparticles revealed monoclinic structure with the major prominent peak at (211) plane, whereas SEM image of the particles showed anisotropic nano rectangular structure and irregular shape. The optical studies demonstrated good absorbance and transmittance within the visible region with direct band gap value in the range of 2.522 eV to 2.547 eV. The electrochemical studies revealed maximum specific capacitance of 1889.31 Fg^{-1} , energy and power density at 9.64 Whkg^{-1} and 1260.13 Wkg^{-1} , respectively for the synthesized nanoparticles.

Graphical Abstract



Introduction

Research has shown that the increased collapse of fossil fuels, emission of greenhouse gases and rapid growth in the world population is highly demanding for renewable energy development and energy storage devices. To address this issue, tremendous research on the production of alternative storing systems of energy is highly needed [1] as a reliable means to cease the shortage of energy. Energy is very critical to any country's advancement, poverty eradication, development and economic growth at large [2]. Storing systems that possess high power and energy densities such as supercapacitors have triggered enormous research [3]. The continuous demand for environmentally friendly and cost-effective energy has been generated through the development of storage devices [4]. Present technology has extensively gone deep into nanotechnology commercialization owing to its broad applications [5–9] in supercapacitors

[10], phototransistors [11], lithium-ion batteries [12], sensor [13], energy conversion and storage devices [14], transistors [15], photocatalysis [16], DNA sequencer [17], photodetectors [18], etc.

Supercapacitors also known as electrochemical capacitors are potential energy storage devices for portable systems and hybrid electric vehicles owing to their superior power density (about $500\text{--}10,000 \text{ KWkg}^{-1}$), long cycling lives (about $10^5\text{--}10^6$ cycles), and abilities of fast energy storage [3, 19–21]. It has also shown excellent applications in military devices, memory backup systems, airbags, load cranes and other interesting areas [22–25]. Supercapacitors have proven to be viable replacement of fuel cells and batteries due to its superior qualities in scientific and engineering applications [26]. It is an interesting area in the recent time due their unique properties such as small charge time, non-toxic, small weight, and other excellent qualities. Supercapacitors have a larger energy

storage capacity and lower equivalent series resistance than regular electrolytic capacitors and they have shown excellent characteristics [27] in energy production [28].

Materials based on cobalt phosphates and cobalt oxides have drawn great interest due to their potential applications in technology and scientific fields [29]. Cobalt phosphate is widely utilized in energy fabrication devices due to its unique properties and applications generally [30], pigments and coatings, chemical manufacturing, and biomedical. Transition metal phosphates have shown excellent performance in many industrial areas [19] and proven to be good in energy storage and other related areas also. Owing to their catalytic efficiency and excellent stability, transition metals phosphates have sparked widespread

interest in energy conversion and storage applications in recent years [31, 32].

In this work, we synthesized cobalt phosphate nanoparticles using co-precipitation method of extraction as shown in Figure 1. The cobalt phosphates nanoparticles were prepared at various molar concentrations ranging from 0.1 M – 0.5 M. Co-precipitation method of extraction is a simple chemical route which involves the precipitation of a solid from a solution containing other ions [33] as shown in Figure 1. In fact, this method of extraction is very simple to apply and inexpensive [34] when compared to other method of extraction techniques. Many research works have shown that co-precipitation method of extracting nanoparticles is the classic method for production of cobalt phosphates nanoparticles [35].

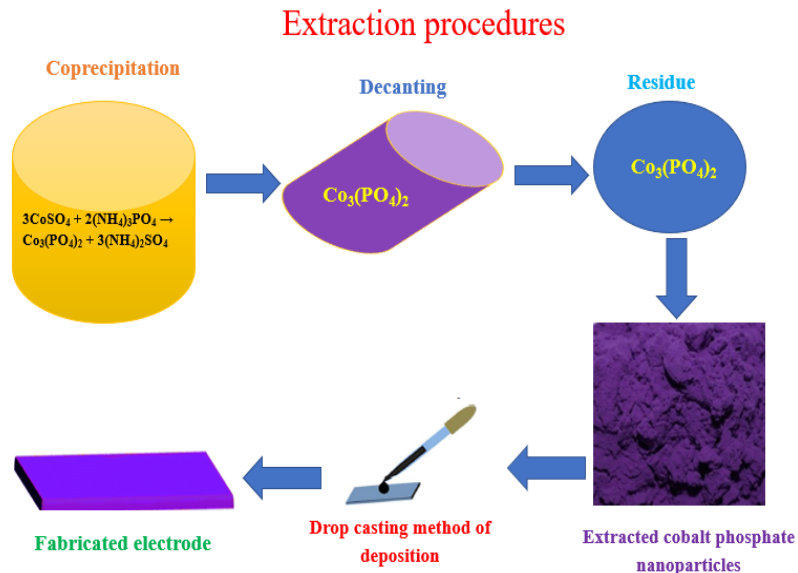


Figure 1. Schematic diagram for the extraction of cobalt phosphate nanoparticles

Drop-casting method of deposition was employed for fabrication of the electrodes. Drop-casting is simply the method of depositing thin films and nanoparticles onto a substrate or electrode by allowing the drops on the substrates. This method of fabrication of

electrodes is capable of creating good quality, uniform nanoparticles for a variety of applications [36]. The morphological and structural properties were studied using scanning electron microscopy (SEM) and X-ray diffractometry (XRD). The optical and

electrochemical properties of the deposited cobalt phosphate nanoparticles were studied using UV-vis spectroscopy and a 3-electrode potentiostat correspondingly.

Experimental

Materials and methods

All the chemicals used in this work, such as cobalt sulfate heptahydrate ($\text{CoSO}_4 \cdot 7\text{H}_2\text{O}$), ammonium phosphate ($(\text{NH}_4)_3\text{PO}_4$) and sodium sulfate (Na_2SO_4) were of analytical grade 99.99% purity and required no further purification. Distilled water was used in this work throughout the experimental procedures. The substrates used were glass and stainless electrodes. The particles extracted were deposited on the stainless and glass substrates respectively. We used stainless substrates for electrochemical studies and glass substrate for optical studies. The nanoparticles of the extracted cobalt phosphate were used for SEM and XRD studies. The glass and stainless substrates were cleaned by soaking them in a beaker filled with distilled water and detergent. The substrates were later ultrasonicated in acetone for 1 hr. Distilled water was used to rinse the substrates immediately they were removed from ultrasonic machine. The substrates were allowed for air-drying for 24 hours before deposition.

Synthesis of cobalt phosphate nanoparticles

We synthesized cobalt phosphate nanoparticles of which five molarities of the solutions labeled 0.1 M, 0.2 M, 0.3 M, 0.4 M, and 0.5 M respectively were prepared by mixing the individually-calculated amounts of cobalt sulfate heptahydrate ($\text{CoSO}_4 \cdot 7\text{H}_2\text{O}$) and ammonium phosphate ($(\text{NH}_4)_3\text{PO}_4$) with 70 mL of distilled water in a 100 mL beaker volume. The individual amounts of the reagents used were

obtained stoichiometrically. 0.1 M – 0.5 M of the mixed solutions were stirred continuously for an hour using a magnetic stirrer at temperature range of 60 °C till homogenous solutions were obtained. Solutions were allowed to settle for 12 hours before decanting it to collect the residual (nanoparticle). The extracted nanoparticles of various molarities were dried in an oven for 2 hours. The extracted cobalt phosphate nanoparticles were later transferred to a thermostatic blast resettable oven for annealing at 300 °C for 3 hours.

Characterization

The morphological investigation of the cobalt phosphate ($\text{Co}_3(\text{PO}_4)_2$) nanoparticles were carried out using a scanning electron microscope (SEM). The crystallinity, crystallite sizes, and crystal phases were determined by X-ray powder diffractometer (XRD). The energy dispersive X-ray spectroscopy (EDX) analysis was also employed in the study to confirm the elemental composition of cobalt phosphates nanoparticles. The UV-Vis spectrophotometer was employed to study the optical properties of cobalt phosphate ($\text{Co}_3(\text{PO}_4)_2$) nanoparticles. Furthermore, electrochemical experimental analysis in a three-electrode system was used to determine the specific capacitance, energy density and power density through cyclic voltammetry (CV), galvanostatic charge-discharge (GCD) and electrochemical impedance spectroscopy (EIS).

Results and Discussion

Structural studies

Figure 2 demonstrates the X-ray diffractogram for the prepared cobalt phosphate nanoparticles with JCPDS number: 13-0503. The nanoparticles were monoclinic crystals which is in agreement with the work

done by [37] on cobalt phosphate nanoparticles. The XRD plots revealed that the highest peak occurred at the reflection plane of (2 1 1) at a 2theta angle of 30.2°. Lattice planes of (2 0 0), (1 0 1), (0 3 1), (3 2 1), (1 4 1), (3 0 1), (0 5 1) and (3 4 1) were observed at 2theta angles of 18.2, 23.2, 28.0, 33.2, 33.4, 37.4, 39.1, and 40.8° respectively. It was also observed in the XRD plots that 0.3 M concentration exhibited amorphous structure as there was no indication of any peak in the plot. This indication of amorphous nature in 0.3 M is in agreement with the work done by [38] on cobalt phosphate nanoparticles. Full width at half maximum

(FWHM) values of the samples was obtained for the most prominent peaks as outlined in Table 1. The crystallite sizes and dislocation densities of the nanoparticles were obtained using equations (1-2) [39, 40].

$$D = k\lambda / \beta \cos\theta \quad (1)$$

$$\delta = 1 / D^2 \quad (2)$$

It is evident from Table 1 that increasing the molar concentrations led to decreasing crystallite sizes of the cobalt phosphate nanoparticles. The lattice planes and corresponding 2theta angles for the as-deposited materials have also been outlined.

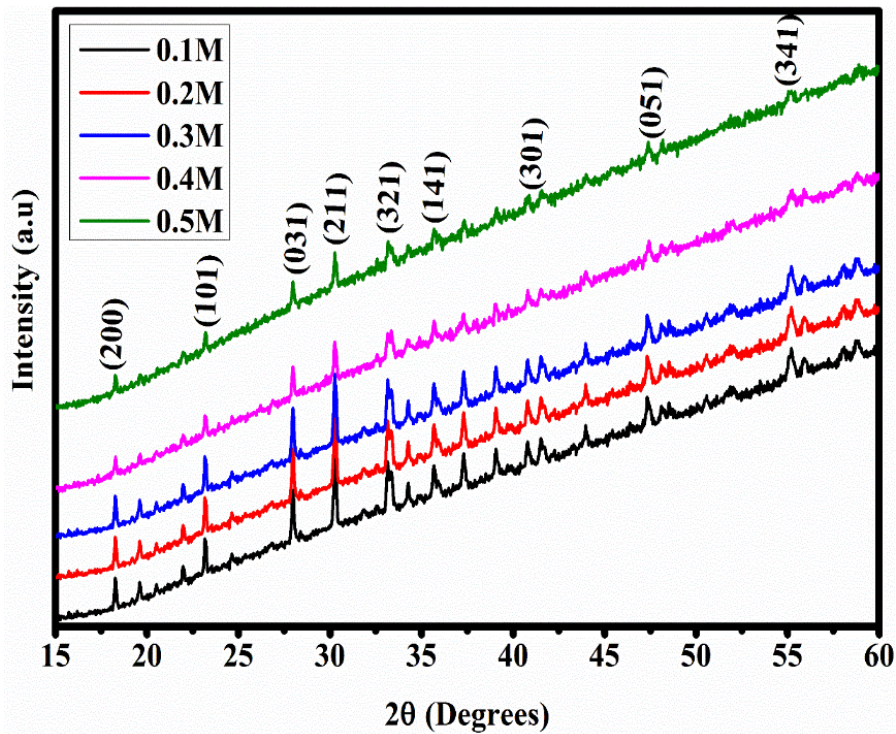


Figure 2. XRD pattern of cobalt phosphate nanoparticles

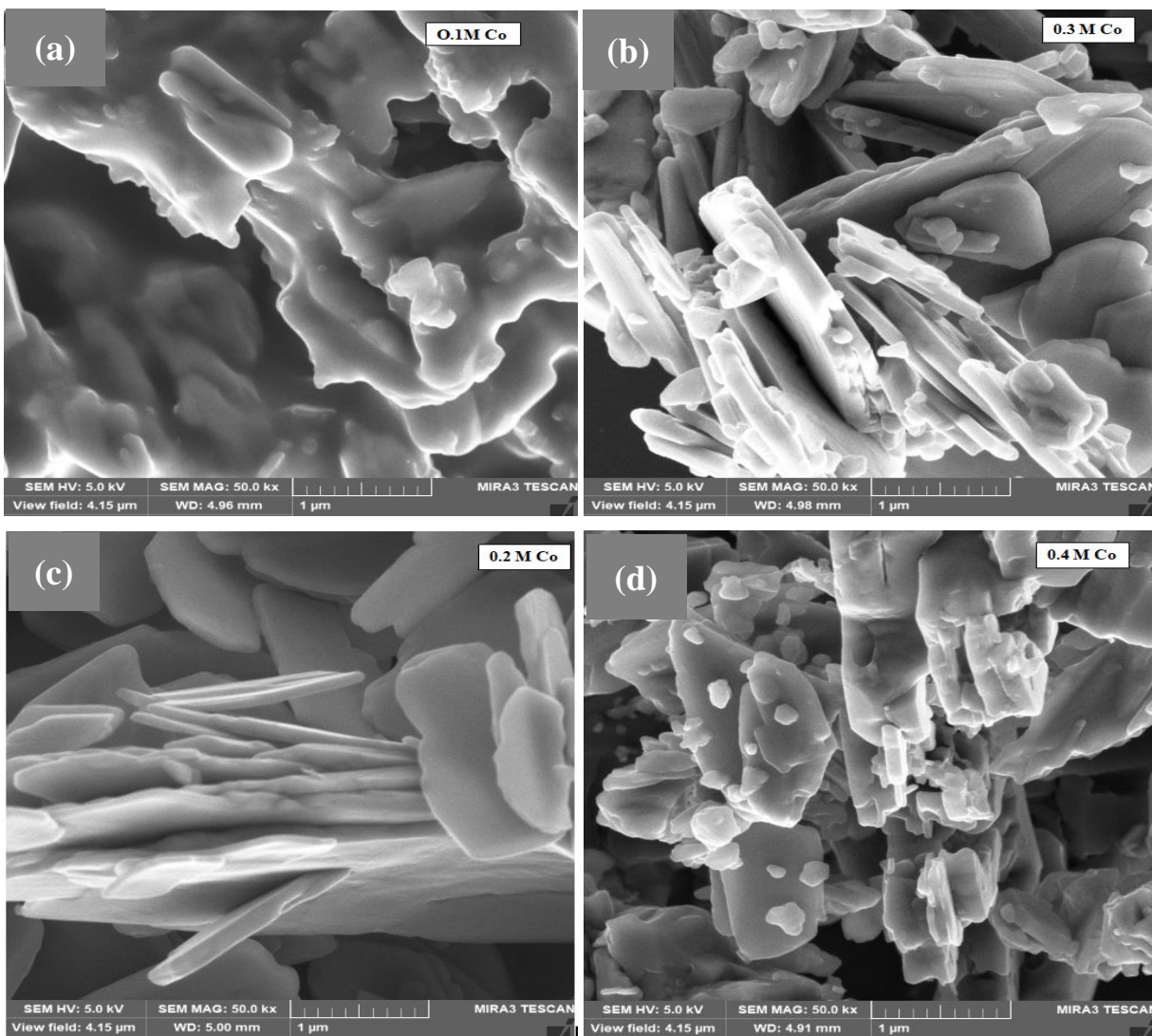
Table 1. Some calculated values on the structure of the nanoparticles

Samples	2θ (°)	(hkl)	FWHM	D (nm)	Dislocation density, δ
0.1 M	18.2	2 0 0	0.0048	30.54	0.0011
0.2 M	23.2	1 0 1	0.0041	36.04	0.0008
0.3 M	28.0	0 3 1	0.0033	45.21	0.0005
0.4 M	30.2	2 1 1	0.0027	55.53	0.0003
0.5 M	33.2	3 2 1	0.0023	65.68	0.0002

Morphological studies

The surface morphology of the nanoparticle was studied using a MIRA3 TESCAN scanning electron microscope (SEM) at an accelerating voltage of 5.0 kV. The morphology and nano-scale particles size are critical aspects in understanding bulk materials properties [41]. The SEM images of cobalt phosphate ($\text{Co}_3(\text{PO}_4)_2$) nanoparticles for varying precursor molarities are presented in

Figure 3. It can be observed from the surface morphology that the cobalt phosphate ($\text{Co}_3(\text{PO}_4)_2$) nanoparticles revealed anisotropic nano rectangular morphology for different concentrations. The surface morphologies are similar to those obtained by [38]. The results obtained showed that 0.3 M, 0.4 M and 0.5 M displayed more irregular shape than that of 0.1 M and 0.2 M which could be as a result of high temperature annealing and high concentration in molarities.



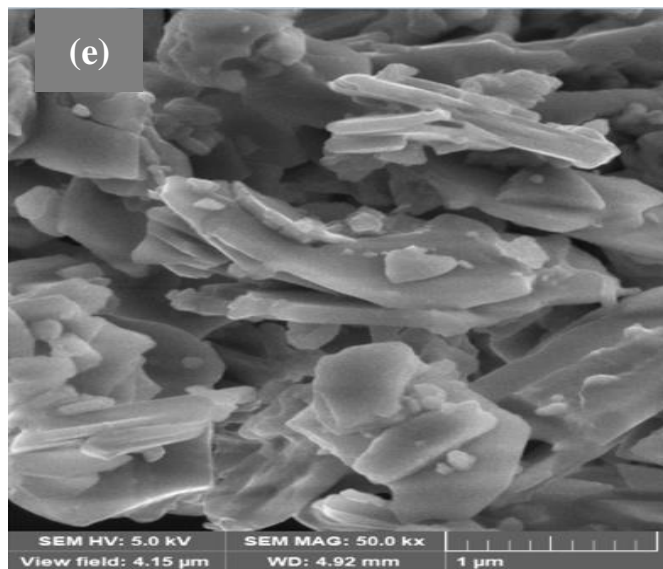


Figure 3. SEM images of cobalt phosphate ($\text{Co}_3(\text{PO}_4)_2$) films (electrodes) a) 0.1 M b) 0.2 M c) 0.3 M d) 0.4 M and e) 0.5 M

Energy dispersive X-ray spectroscopy (EDS)

Figure 4 shows the energy dispersive spectra of cobalt phosphate nanoparticles. The plots reveal that the major elements: cobalt (Co), oxygen (O) and phosphorous (P) were confirmed as constituents of the fabricated nanoparticles using energy dispersive X-ray spectroscopy as shown in Figure 4a–e. The EDS analysis displayed quantitative composition of the elements fabricated on the substrate in order of their different energies. Other elements such as carbon, sulfur, potassium, and calcium that were observed could be as a result of the composition of the elements associated with the substrate and laboratory instruments used during the extraction of the particles.

Optical studies

The plots of absorbance against wavelength of cobalt phosphate ($\text{Co}_3(\text{PO}_4)_2$) nanoparticles of various molarities are shown in Figure 5. The absorbance was studied using a UV-vis

spectrophotometer (UV-7504) and recorded in the wavelength range between 200 nm to 800 nm to cover the ultraviolet (UV), visible (Vis) and near-infrared (NIR) regions of the electromagnetic spectrum. The deposited nanoparticles exhibited high absorbance in the UV region of the electromagnetic spectrum with sharp drop within the visible region and very low absorbance towards the NIR region. It can be shown that the sample has high absorbance within the visible region of the electromagnetic spectrum. The particle has about 60% absorbance within the visible region but decreased to about 30% towards the NIR region. The highest absorbance in the visible region was recorded by 0.5 M while that with the highest absorbance in the infrared region was recorded by 0.2 M. This excellent property suggests that cobalt phosphate ($\text{Co}_3(\text{PO}_4)_2$) nanoparticles could be applied as photoelectrodes owing to its higher absorbance in the visible and NIR region. Table 2 shows the various absorbance values of the samples at different molarities.

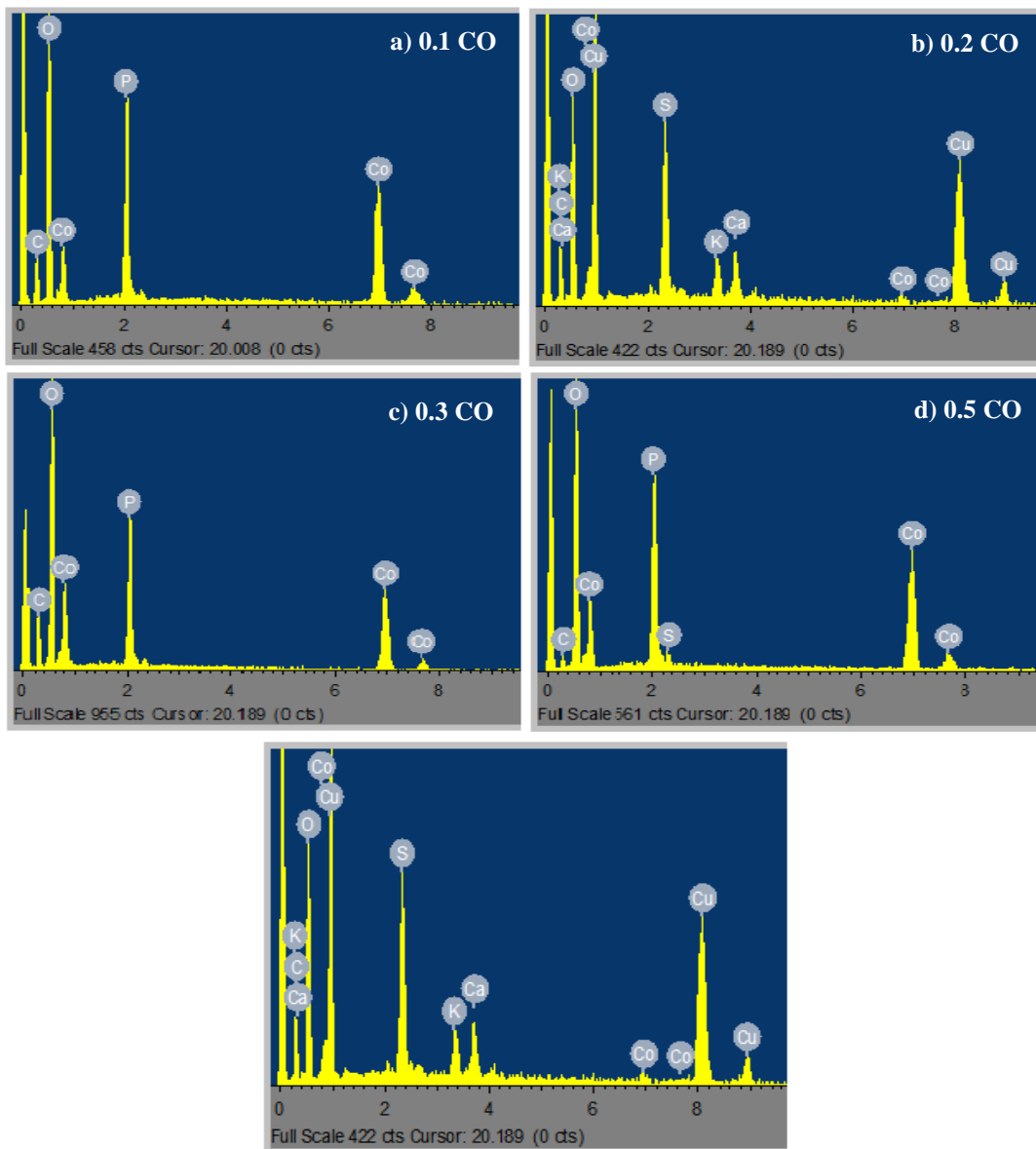


Figure 4. EDS Spectrum for cobalt phosphate nanoparticles

Figure 5. Plots of the absorbance against wavelength of cobalt phosphate ($\text{Co}_3(\text{PO}_4)_2$) nanoparticles

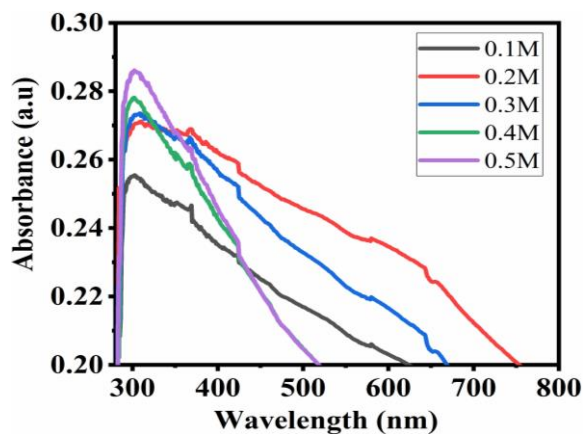


Figure 6 shows the band gap energy of the various molarities of cobalt phosphate nanoparticles. The molarity with highest concentration displayed highest band gap energy. It was also observed that 0.4 M and 0.5 M exhibited similar bandgap energies. The band gap energy ranged from 2.503 eV to 2.547 eV as shown in Table 2. Furthermore, the band gap energies decreased down the concentrations.

Table 2 gives the values of several optical parameters as obtained in the ultraviolet and

near-infrared (NIR) regions. The values of absorbance and transmittance were on the rise at increasing molar concentrations in the ultraviolet spectrum area. At increasing molar concentrations of the samples, their band gap energy values recorded an increasing trend from 1.522 eV to 2.547 eV. Similar band gap energies have also been reported.

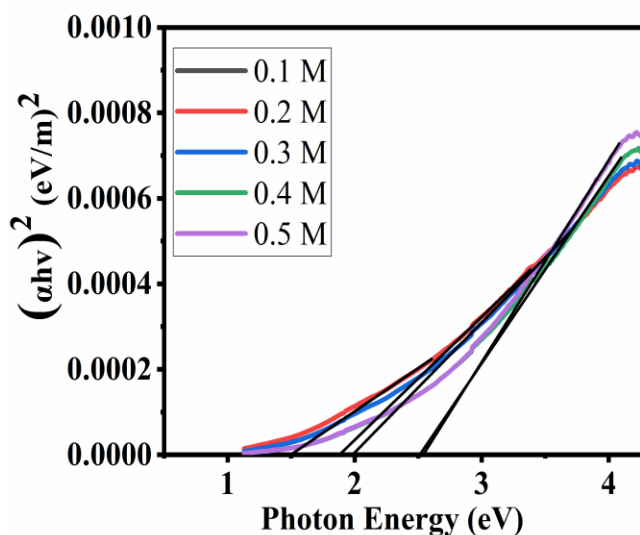


Figure 6. Plots of $(\alpha h\nu)^2$ versus photon energy (eV) to determine the energy band gaps of the deposited cobalt phosphate ($\text{Co}_3(\text{PO}_4)_2$) nanoparticles

Table 2. Summary of optical properties of varying precursor molarities of cobalt phosphate ($\text{Co}_3(\text{PO}_4)_2$) nanoparticles

Molarities	Absorbance		Transmittance		Band gap energy (eV)
	UV	Visible	UV	Visible	
0.1 M	0.255	0.217	0.542	0.712	1.522
0.2 M	0.270	0.246	0.542	0.712	1.898
0.3 M	0.273	0.233	0.533	0.773	1.995
0.4 M	0.277	0.205	0.528	0.838	2.503
0.5 M	0.286	0.205	0.518	0.846	2.547

Electrochemical studies

Cyclic Voltammetry

A 3-electrode potentiostat was adopted in understanding the electrochemical properties

of the cobalt phosphate ($\text{Co}_3(\text{PO}_4)_2$) nanoparticles synthesized on stainless electrodes. The scan was carried out at five (5) varying rates of 5 mV/s, 10 mV/s, 20 mV/s, 30 mV/s and 40 mV/s at a potential window of 0.0 to 0.7 V for the five electrodes. Ag/AgCl served

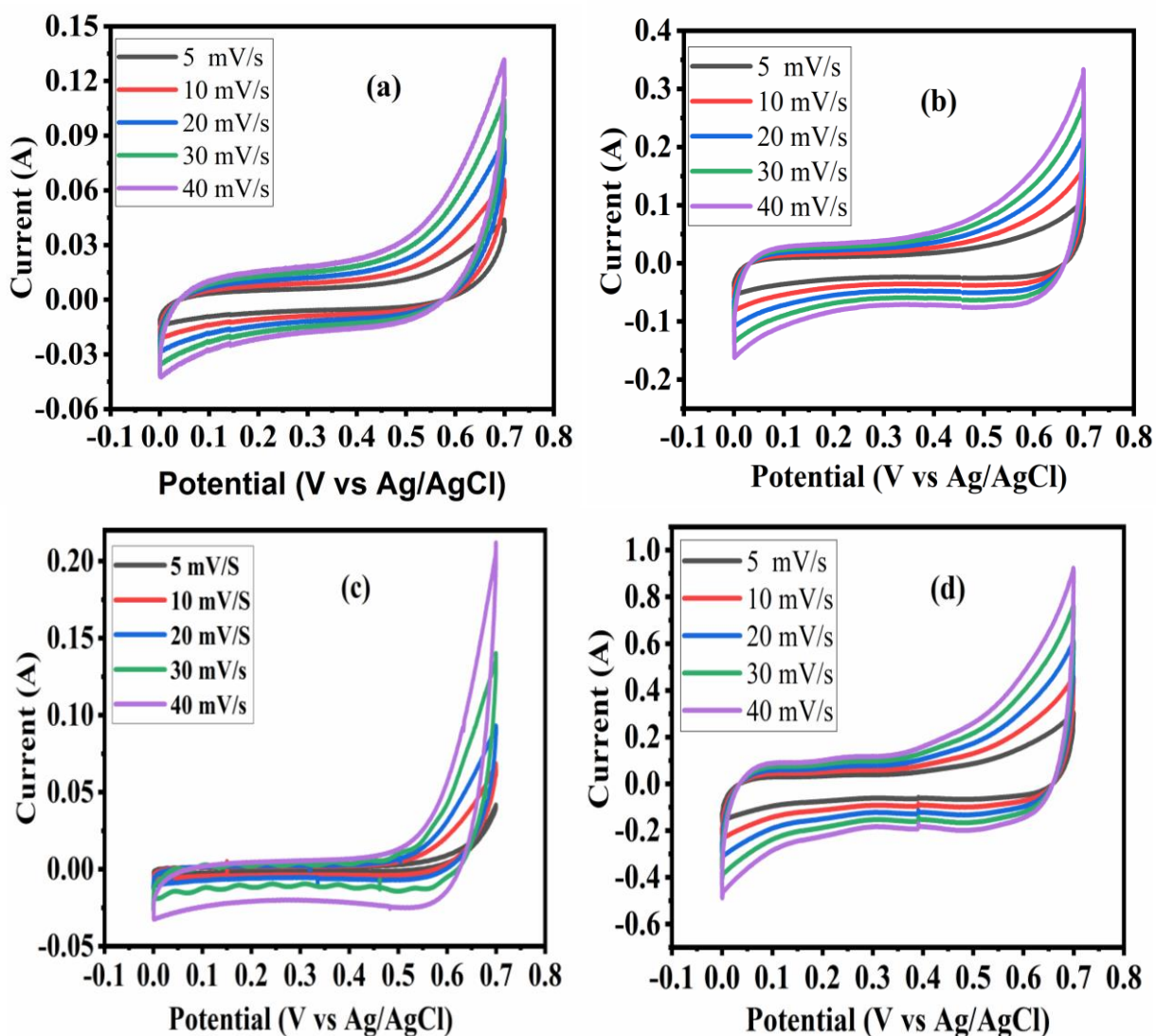
as the reference electrode, cobalt phosphate ($\text{Co}_3(\text{PO}_4)_2$) nanoparticle was the working electrode, while carbon electrode served as the counter electrode. The specific capacitance (C_s) of the five electrodes as studied was obtained from the cyclic voltammetry (CV) plots in Figure 7 using equation (3) [42, 43].

$$C_{\text{sp}} = \frac{1}{mVs} \int i(V)dV \quad (\text{F/g}) \quad (3)$$

Where m is the active mass in mg, V is the potential window used in volts, S is the scan rate

in mV/s and i is the current applied in ampere (A). Figure 7 shows pseudocapacitive behavior with distinct redox peaks shown for synthesized electrodes [44].

The calculated specific capacitance of various fabricated electrodes using 5.0 mV/s scan rate, which is the scan rate with highest specific capacitance are 296, 308, 339, 358 and 491 F/g for 0.1, 0.2, 0.3, 0.4 and 0.5 M respectively. These results are in good agreement with reference [42].



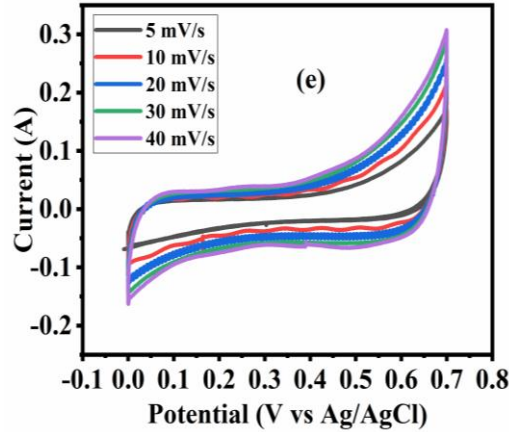


Figure 7. Cyclic voltammetry plots for a) 0.1 M b) 0.2 M c) 0.3 M d) 0.4 M and e) 0.5 M of cobalt phosphate ($\text{Co}_3(\text{PO}_4)_2$) nanoparticles

Alvanostatic charge and discharge

Figure 8 illustrates the GCD plots of cobalt phosphate ($\text{Co}_3(\text{PO}_4)_2$) nanoparticles at a current density of 1.0 A/g. As observed, the scanning potential increases with time until after 60 s when the potential declined over time. Table 3 displays the specific capacitance values and their corresponding energy density and power density values. GCD measurements were adopted because electrode stability is essential for usage as electrochemical capacitors [45]. The specific capacitance (C_s), energy density (E_d) and power density (P_d) values were respectively determined using equations (4-6) [46].

$$C_s = \frac{I}{m \frac{dV}{dt}} \quad (4)$$

$$E_d = 0.5C_s(\Delta V)^2 \quad (5)$$

$$P_d = 3.6 \frac{E_d}{t_d} \quad (6)$$

Where ΔV is the potential window and t_d stands for the time taken to discharge.

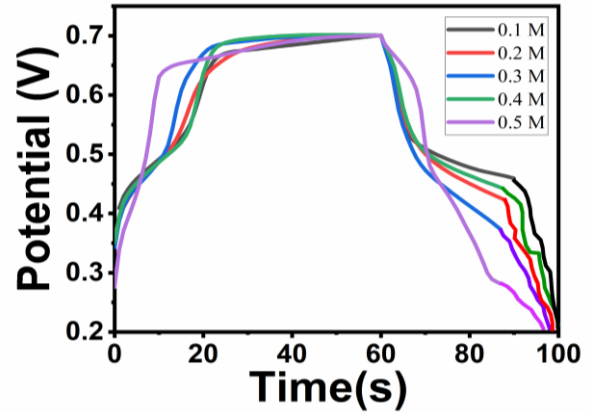


Figure 8. Galvanostatic charge-discharge plots of various concentration of cobalt phosphate ($\text{Co}_3(\text{PO}_4)_2$) nanoparticles

Table 3. Specific capacitance, energy density, and power density values obtained from GCD measurements

S/N	Molarity	Specific capacitance (F/g)	Energy density (Wh/kg)	Power density (W/kg)
1	0.1	228	55.86	2.79
2	0.2	294	72.03	10.29
3	0.3	346	84.77	10.59
4	0.4	398	97.51	14.38
5	0.5	418	102.41	17.06

Electrochemical impedance spectroscopy

EIS analysis is essential in studying the capacitive behavior of the samples for range of frequency values from 1.0 Hz to 100 kHz. It is necessary as the rate of emitting power for

electrochemical capacitors depends on the electrode impedance [47]. The EIS plots in Figure 9 show that cobalt phosphate ($\text{Co}_3(\text{PO}_4)_2$) nanoparticles have high conductivity and low resistance properties.

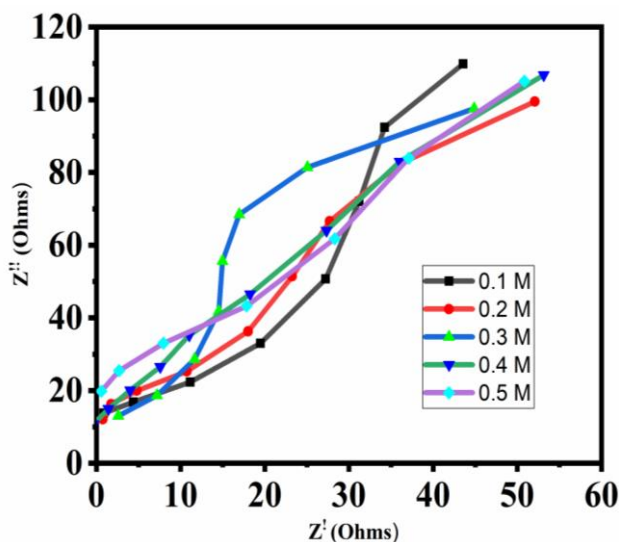


Figure 9. Electrochemical impedance spectroscopy of 0.1 M – 0.5 M of cobalt phosphate ($\text{Co}_3(\text{PO}_4)_2$) nanoparticles

Conclusions

Cobalt phosphate ($\text{Co}_3(\text{PO}_4)_2$) nanoparticles have been successfully deposited using coprecipitation and followed by drop-casting method. SEM, XRD, EDS, UV-vis spectrophotometry, and electrochemical characterizations were employed in understanding the morphological, structural, elemental, optical, and electrochemical features of the synthesized nanoparticles. The surface morphologies exhibited irregular nanorectangular shapes with prominent peaks observed from the structural analysis. The most prominent peak was observed at (2 1 1) lattice plane. EDX analysis confirmed the deposition of constituent elements. Optical studies showed increasing band gap energies (in the range of 1.522 eV to 2.547 eV) at increasing molar concentrations. Other optical parameters such as absorbance, transmittance, and energy band

gap values were also determined. The electrochemical properties of the prepared electrodes gave good charge storage features. The synthesized nanoparticles find potential application in supercapacitors and solar cells.

Acknowledgements

RMO humbly acknowledges NCP for their PhD fellowship (NCP-CAAD/PhD-132/EPD) award and COMSATS for travel grant for the fellowship. FIE graciously acknowledge the grant by TETFUND under contract number TETFUND/DR&D/CE/UNI/NSUKKA/RP/VOL.1 and also acknowledge the support received from the Africa Centre of Excellence for Sustainable Power and Energy Development (ACE-SPED), University of Nigeria, Nsukka that enabled the timely completion of this research. We thank Engr. Emeka Okwuosa for the generous sponsorship of April 2014, July 2016,

July 2018 and July 2021 conferences/workshops on applications of nanotechnology to energy, health & Environment and for providing some research facilities.

Disclosure Statement

No potential conflict of interest was reported by the authors.

References

- [1]. Radhamani A. V., Ramachandra Rao M. S. *Applied Surface Science*, 2017, **403**:601
- [2]. Oyedepo S.O. *Energy, Sustainability and Society*, 2012:15
- [3]. Deng J., Kang L., Bai G., Li Y., Li P., Liu X., Yang Y., Gao F., Liang W. *Electrochimica Acta*, 2014, **132**:127
- [4]. Nwanya A.C., Obi D., Ozoemena K.I., Osuji R.U., Awada C., Ruediger A., Maaza M., Rosei, F., Ezema, F. I. *Electrochimica Acta*, 2016, **198**:220
- [5]. Wang X., Ma L., Sun J. *International Journal of Energy Research*, 2019, **43**:9025
- [6]. Azman N.H.N., Mamat @ Mat Nazir M.S., Ngee L.H., Sulaiman Y. *International Journal of Energy Research*, 2018, **42**:2104
- [7]. Rafique M., Sadaf I., Nabi G., Bilal Tahir M., Khan M.I. *International Journal of Energy Research*, 2019, **43**:2361
- [8]. Obodo R.M., Nwanya A.C., Iroegbu C., Ahmad I., Ekwealor A.B.C., Osuji R.U., Maaza M., Ezema F.I. *International Journal of Energy Research*, 2020, **44**:6792
- [9]. Linghao S.U., Liangyu Gong X.W., *Archives of Thermodynamics*, 2012, **33**:23
- [10]. Mao S., Wen Z., Kim H., Lu G., Hurley P., Chen J. *ACS Nano*, 2012, **6**:7505
- [11]. Nkelea A.C., Nwanya A.C., Nwankwoa N.U., Ekwealora A.B.C., Osujia R.U., Bucher R., Maaza M., Ezema F.I. *Materials Research Express*, 2019, **6**:096439
- [12]. Wang D., Kou R., Choi D., Yang Z., Nie Z., Li J., Saraf L. V., Hu D., Zhang J., Graff G. L., Liu J., Pope M.A., Aksay I.A. *ACS Nano*, 2010, **4**:1587
- [13]. Deb S.K. *Solar Energy Materials and Solar Cells*, 2008, **92**:245
- [14]. Huang Q., Zeng D., Li H., Xie C. *Nanoscale*, 2012, **4**:5651
- [15]. Fiori G., Bonaccorso F., Iannaccone G., Palacios T., Neumaier D., Seabaugh A., Banerjee S.K., Colombo L. *Nature Nanotechnology*, 2014, **9**:768
- [16]. Wang J., Tsuzuki T., Tang B., Hou X., Sun L., Wang X. *ACS Applied Materials and Interfaces*, 2012, **4**:3084
- [17]. Thomas S., Rajan A.C., Rezapour M.R., Kim K.S. *Journal of Physical Chemistry C*, 2014, **118**:10855
- [18]. Koppens F.H.L., Mueller T., Avouris P., Ferrari A.C., Vitiello M.S., Polini M. *Nature Nanotechnology*, 2014, **9**:780
- [19]. Li B., Gu P., Feng Y., Zhang G., Huang K., Xue H., Pang H. *Advanced Functional Materials*, 2017, **27**:1605784
- [20]. Hsu S.H., Li C.T., Chien H.T., Salunkhe R.R., Suzuki N., Yamauchi Y., Ho K.C., Wu K.C.W. *Scientific Reports*, 2014, **4**:1
- [21]. Ighodalo K.O., Ezealigo B.N., Agbogu A., Nwanya A.C., Obi D., Mammah S.L., Botha S., Bucher R., Maaza M., Ezema F.I. *Materials Science in Semiconductor Processing*, 2019, **101**:16
- [22]. Yang Y., Han C., Jiang B., Iocozzia J., He C., Shi D., Jiang T., Lin Z. *Materials Science and Engineering R: Reports*, 2016, **102**:1
- [23]. Theerthagiri J., Thiagarajan K., Senthilkumar B., Khan Z., Senthil R.A., Arunachalam P., Madhavan J., Ashokkumar M. *Chemistry Select*, 2017, **2**:201
- [24]. Tang P., Han L., Zhang L., Wang S., Feng W., Xu G., Zhang L. *Chem Electro Chem*, 2015, **2**:949
- [25]. Ji J., Zhang L.L., Ji H., Li Y., Zhao X., Bai X., Fan X., Zhang F., Ruoff R.S. *ACS Nano*, 2013, **7**:6237
- [26]. Obodo R.M., Nwanya A.C., Ekwealor A.B.C., Ahmad I., Zhao T., Osuji R.U., MaazaM., Ezema F.I. *Surfaces and Interfaces*, 2019, **16**:114
- [27]. Obodo R.M., Onah E.O., Nsude H.E., Agbogu A., Nwanya A.C., Ahmad I., Zhao T., Ejikeme P.M., Maaza M., Ezema F.I. *Electroanalysis*, 2020, **32**:2786
- [28]. Obodo R.M., Nwanya A.C., Arshad M., Iroegbu C., Ahmad I., Osuji R.U., Maaza M., Ezema F.I. *International Journal of Energy Research*, 2020, **44**:3192

- [29]. Barreca D., Massignan C., Inorganica C., Analitica M., Loredan V., Padova I., Barreca D., Massignan C., Daolio S., Fabrizio M., Piccirillo C., Armelao L., Tondello E. *Chem. Mater.* 2001, **13**:588
- [30]. Badsar M., Edrissi M. *Materials Research Bulletin*, 2010, **45**:1080
- [31]. Xuan L.L., Liu X.J., Wang X. *Frontiers in Materials*, 2019, **6**:1
- [32]. Zhou T., Du Y., Yin S., Tian X., Yang H., Wang X., Liu B., Zheng H., Qiao S., Xu R. *Energy and Environmental Science.*, 2016, **9**:2563
- [33]. Badsar M., Edrissi M. *Materials Research Bulletin*, 2010, **9**:1080
- [34]. Pudovkin M.S., Zelenikhin P.V., Shtyryeva V., Morozov O.A., Koryakovtseva D.A., Pavlov V.V., Osin Y.N., Evtugyn V.J., Akhmadeev A.A., Nizamutdinov A.S., Semashko V.V. *Journal of Nanotechnology*, 2018, **2018**:9 pages
- [35]. Zhou G., Wang W., Gu G., Li Y., Liu Y. *International Journal of Chemistry*, 2011, **4**:127
- [36]. Eslamian M., Soltani-Kordshuli F. *Journal of Coatings Technology & Research*, 2018, **15**:271
- [37]. Zhou G., Wang W., Gu G., Li Y., Liu Y. *International Journal of Chemistry*, 2011, **3**:127
- [38]. Duraisamy N., Arshid N., Kandiah K., Iqbal J., Arunachalam P. *Journal of Materials Science: Materials in Electronics*, 2019, **30**: 7435
- [39]. Nkele A.C., Chime U.K., Asogwa L., Nwanya A.C., Nwankwo U., Ukoba K., Jen T.C., Maaza M., Ezema F.I. *Inorganic Chemistry Communications.*, 2020, **112**:107705
- [40]. Nkele A.C., Nwanya A.C., Nwankwo N.U., Osuji R.U., Ekwealor A.B.C., Ejikeme P.M., Maaza M., Ezema F.I. *Adv Nat Sci: Nanosci Nanotechnol*, 2019, **10**:045009
- [41]. Sajid S., Elseman A.M., Huang H., Ji J., Dou S., Jiang H., Liu CX., Wei D., Cui P., Li M. *Nano Energy*, 2018, **51**:408
- [42]. Nkele A.C., Chime U.K., Nwanya A.C., Obi D., Osuji R.U., Bucher R. Ejikeme P.M., Maaza M., Ezema F.I. *Vacuum*, 2019, **161**:306
- [43]. Nkele A.C., Chime U., Ezealigo B., Nwanya A., Agbogu Ada N.C., Ekwealor A.B.C., Osuji R.U., Ejikeme P.M., Maaza M., Ezema F.I. *Journal of Materials Research and Technology.*, 2020, **9**:9049
- [44]. Kim T., Tiwari A.P., Chhetri K., Ojha G.P., Kim H., Chae S.H., Dahal B., Lee B.M., Mukhiya T., Kim H.Y. *Nanoscale Advances.*, 2020, **2**:4918
- [45]. Iqbal M.Z., Khan J., Afzal A.M., Aftab S. *Electrochimica Acta.*, 2021, **384**:138358
- [46]. Maher M., Hassan S., Shoueir K., Yousif B., Abo-ElSoud M.E.A. *Journal of Materials Research and Technology*, 2021, **11**:1232
- [47]. Iqbal M.Z., Khan J., Siddique S., Afzal A.M., Aftab S. *International Journal of Hydrogen Energy*, 2021, **46**:15807

How to cite this manuscript: Jude N. Udeh, Agnes C. Nkele*, Raphael M. Obodo, Innocent C. Nwodo, Chinedu P. Chime, Assumpta C. Nwanya, Malik Maaza, Fabian I. Ezema. Investigating the properties of cobalt phosphate nanoparticles synthesized by co-precipitation method. *Journal of Medicinal and Nanomaterials Chemistry*, 4(1) 2022, 22-35. DOI: [10.48309/jmnc.2022.1.3](https://doi.org/10.48309/jmnc.2022.1.3)